Journal of Power Sources 222 (2013) 470–476

Contents lists available at SciVerse ScienceDirect

Journal of Power Sources

journal homepage: www.elsevier.com/locate/jpowsour

Mitigating methanol crossover with self-assembled Pt_{35}–Ru_{65} catalyst on Nafion surface

Chieh-Hao Wan [a,*], Meng-Tsun Lin [b]

[a] Department of Electro-Optical and Energy Engineering, MingDao University, Taiwan, ROC
[b] Department of Materials Science and Engineering, National Chung Hsing University, Taiwan, ROC

HIGHLIGHTS

- A new approach to mitigate methanol crossover has been proposed.
- A layer of Pt_{35}–Ru_{65} with a thickness of 87.5 nm deposited on Nafion acts as a methanol barrier.
- MEA with self-assembled Pt_{35}–Ru_{65} layers suppresses methanol crossover by 22% and improves power density by 48% (at 0.30V) at 80 °C.
- Catalytic reaction, microstructure and low methanol permeability of self-assembly layers affect methanol crossover.

ARTICLE INFO

Article history:
Received 1 July 2012
Received in revised form
23 August 2012
Accepted 27 August 2012
Available online 7 September 2012

Keywords:
Self-assembly membrane
Methanol crossover
Nanometer-sized catalyst
Layer-by-layer technique
Mixture potential effect

ABSTRACT

In this paper, 5 bi-layers of poly (allylamine hydrochloride) (PAH)/polystyrene sulfonic acid sodium salt (PSS) containing Pt_{35}–Ru_{65} catalyst are self-assembled on the Nafion membrane surface through the layer-by-layer technique to mitigate methanol crossover. This composite Nafion membrane coated with Pt_{35}–Ru_{65} catalyst with loading of 0.46 μg cm^{-2} and layer thickness of 87.5 nm on both surfaces suppresses the methanol crossover by 22% (on average), improves the power density by 48% (@0.30 V) and the potential by 22% (@62.5 mA cm^{-2}) at 80 °C. The Pt_{35}–Ru_{65} catalyst in the PAH/PSS bi-layers serves multiple roles at the same time – a catalytically active layer, a methanol barrier and an electrode. In addition, the PAH/PSS bi-layers also acts as a methanol barrier. These roles contribute to the suppression of methanol crossover and improvement of the output performance. Compared with Pt–Ru directly deposited on Nafion surface, the deposition of Pt_{35}–Ru_{65} in this study has less negative impact on the cell performance because 1) lesser and thinner deposited Pt_{35}–Ru_{65} is used, 2) the Pt_{35}–Ru_{65} layer deposited on the additional PAH/PSS bi-layers does not reduce the proton conductivity of Nafion membrane.

1. Introduction

Direct methanol fuel cells (DMFCs) are attractive in portable and transportation applications due to its high energy density and simple system design [1–3]. However, two major challenges should be addressed to increase the efficiency of DMFC before the technology can become commercially viable [4–6]. The first challenge is on developing novel high-activity anode catalyst with appropriate anode structure for direct methanol oxidation. The second challenge is on preventing methanol crossover. Methanol crossover is a process in which un-reacted methanol diffuses from the anode to the cathode through Nafion membrane, and causes the mixed potential effect and poisoning of Pt catalyst at the cathode. As a result, the process significantly reduces the cell performance as well as fuel utilization, particularly for methanol concentration above 3 M [4]. Therefore, it is essential to reduce methanol crossover to increase the efficiency and stability of DMFC.

Several approaches have been proposed to reduce methanol crossover for DMFC during the last decade. The first approach focused on the development of a novel membrane with low methanol permeability and high proton conductivity [7–14], e.g., the acid-doped polybenzimidazole (PBI), sulfonated-poly(arylene ether ketone)s (SPAEKs), sulfonated-poly(ether sulfone)s (SPES), sulfonated-polyimide (SPI), etc. Among them, the aromatic polyethers, which show low methanol permeability with high mechanical and chemical stabilities, are good alternative

* Corresponding author. Tel.: +886 (04) 8876660x8513.
E-mail addresses: n3883115@xuite.net, chiehhao@mdu.edu.tw (C.-H. Wan).

0378-7753/$ – see front matter © 2012 Elsevier B.V. All rights reserved.
http://dx.doi.org/10.1016/j.jpowsour.2012.08.085

candidates for Nafion membrane. The second approach to reduce methanol crossover involved addition of second species into the Nafion membrane to form Nafion-based composite membrane, such as Nafion-zirconium phosphate [15], Nafion-silica [16,17], Nafion-cesium ions [18] and Nafion-poly(furfuryl alcohol) nanocomposite membrane [19]. This approach can drastically reduce the methanol permeability with only slight decrease of proton conductivity. The third approach was the deposition of a Pd layer on a proton exchange membrane (PEM) surface to form a sandwich structure to block the methanol crossover [20,21] at the expense of proton conductivity of Nafion. Alternate approaches for reducing methanol crossover via various techniques to deposit a Pt-based catalyst on Nafion membrane were also investigated. In those studies, the deposition of Pt nanowires [22], a Pt–Ru double layer or a Pt–Sn layer [6,23,24] as well as the dispersion of nanometer-sized Pt particles [25] on the Nafion membrane, were served as the inner catalyst that consumed the crossed-over methanol. It was reported that the methanol crossover was drastically reduced due to its consumption by the inner catalyst while slightly decreasing proton conductivity.

Recently, in Refs. [26–31] coating of various self-assembled layers with low methanol permeability onto the Nafion membrane surface without sacrificing proton conductivity was prepared by the layer-by-layer (LbL) technique to suppress methanol crossover. LbL assembly is a multilayer thin film fabrication method that based on sequential electrostatic adsorption of oppositely charged polyelectrolytes. The support membrane was alternatively dipped into a solution of polycations and polyanions to adsorb the oppositely charged polyelectrolytes onto the surface of membrane. This method is known to well-prepare the composite membrane with an organized, dense and separate self-assembled layer of controlled thickness in the nanometer scale through adjusting assembly parameters such as the pH and ionic strength [31]. P. T. Hammond et al. [32] had demonstrated that the LbL technique could be used to deposit polyelectrolytes and stable carbon colloidal on Nafion surface or porous metal to form a soft membrane electrode assembly (MEA). The resulted LbL electrode, poly(diallyldimethyl ammonium chloride)/poly (2-acrylamido-2-methyl-1-propane sulfonic acid)/carbon–platinum assembled on a porous stainless steel support, had open-circuit voltage similar to that of a pure platinum electrode. Recently, they used the LbL technique to deposit poly(diallyl dimethyl ammonium chloride) (PDAC)/sulfonated poly(2,6-dimethyl 1,4-phenylene oxide) (sPPO) on Nafion membrane to suppress methanol crossover while improving the conductivity of composite membrane [26]. The results showed that 3–5 bi-layers of PDAC/s-PPO could tremendously reduce the methanol permeability down to hundredth while improving performance up to 50% as compared to the untreated Nafion. H. Deligöz et al. [28] had reported that the self-assembly of poly (allylamine hydrochloride) (PAH) and polystyrene sulfonic acid sodium salt (PSS) onto the Nafion membrane reduced the methanol permeability nearly 27% as compared to the unmodified Nafion. When adding 0.01 M NaCl to the PSS solution to produce the PAH/PSS multilayers with extra ions in the polyelectrolyte, the resulted composite membrane achieved 39.9% reduction in methanol permittivity and up to 2 times higher proton conductivity (0.152 S cm^{-1}) than that of the unmodified Nafion-112 [33]. Replacing the PSS polyelectrolyte to the polyvinylsulfate potassium salt (PVS) with 1.0 M NaCl [27], the composite membrane with 10 bi-layers of PAH/PVS in Na^+ and H^+ form offered 55.1% and 43.0% reduction in methanol permittivity as compared to the untreated Nafion, respectively, while the proton conductivities were 12.4 and 78.3 mS cm^{-1}. The result demonstrated that methanol permeability is strongly dependent on the selection of polyelectrolytes.

This paper reports the first-ever effort, to our best knowledge, that uses Nafion membrane surface self-assembly with 5 bi-layers of PAH/PSS with dispersion of Pt_{35}–Ru_{65} catalyst particles via the LbL technique to mitigate methanol crossover and improve cell performance. Fig. 1 shows the structure of PAH/PSS with Pt_{35}–Ru_{65} catalyst coated on Nafion-117 and the corresponding MEA. In this paper, the effects of Pt–Ru catalyst particles in PAH/PSS self-assembled layer on the suppression of methanol crossover and performance improvement are studied. The possible mechanism of suppression of methanol crossover is also investigated.

2. Experimental details

PAH (M_w = 15,000), PSS (M_w = 70,000), and $Pt(NH_3)_4Cl_2$ (supplied from Aldrich) and $Ru[Cl(NH_3)_5]Cl_2$ (supplied from Alfa Aesar) were used as received without further purification. Nafion-117® (DuPont, Inc., USA) with a nominal equivalent weight of 1100 g $equiv^{-1}$ was used as the polymer electrolyte membrane for each sample. Prior to deposition, the membrane was subsequently treated in 3.5% H_2O_2 and 0.5 M H_2SO_4 solution, and finally stored in distilled water. Ultrapure-water, produced using a Milli-Q SP purification system from Nihon Millipore Ltd., Tokyo, was used in all experiments.

2.1. Preparation of Pt_{35}–Ru_{65} catalyst self-assembled on Nafion surface

PAH and PSS were separately dissolved in water in a concentration of 10^{-2} monomol L^{-1}. Monomole represents 1 mol of polyelectrolyte is equal to the weight of one repeating polymer unit. Appropriate amount of $Ru[Cl(NH_3)_5]Cl_2$ and $Pt(NH_3)_4Cl_2$ were added into the PSS solution. The pH of both the PSS and PAH solution were adjusted to 1.8 by adding aqueous HCl. The pre-treated Nafion membrane was dipped into the PAH solution to adsorb the positively charged polyelectrolyte onto the Nafion surface. After rinsing with ultrapure water, the Nafion membrane was dipped into the PSS solution containing the Pt and Ru ions to

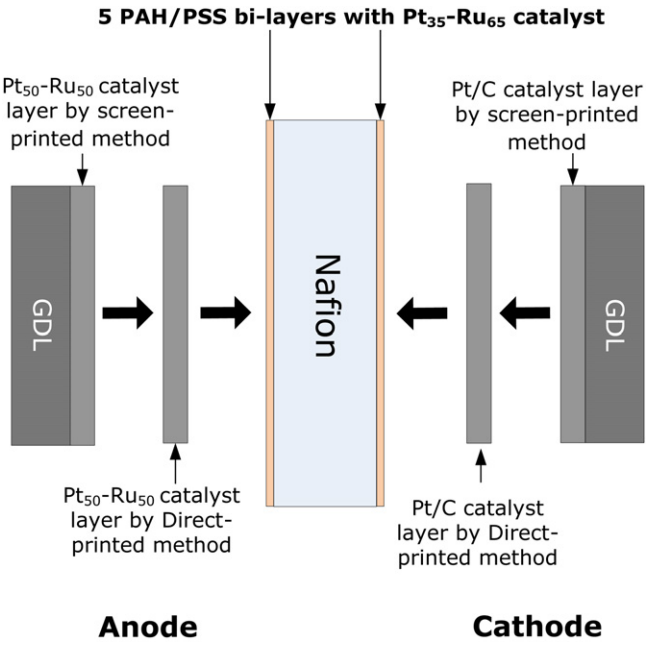

Fig. 1. Diagram of the proposed composite Nafion and corresponding MEA.

deposit the negatively charged polyelectrolyte on the Nafion surface. Dipping process was repeated until the required 5, or 10, 15 bi-layers were formed. These samples were denoted as PAH/PSS–Pt^{+}–Ru^{+}.

PAH/PSS–Pt^{+}–Ru^{+} sample was placed into the reactor with $NaBH_4$ solution to proceed the reduction reactions at 60 °C for 1 h. In order to obtain the fully proton forms of PAH/PSS self assembly layer and Nafion, the resulted sample was treated with 0.50 M H_2SO_4 at 80 °C for 2 h to ion-exchange the un-reacted Pt or Ru ions into the H^{+}. The resulting sample is denoted as PAH/PSS–Pt–Ru.

2.2. Preparation of anode and cathode

Before screen-printing a catalyst layer on the gas diffusion layer (GDL), the carbon cloth (50% wet proof) GDL was screen-printed a backing layer that contained the carbon powder (Vulcan XC-72) and 5% Nafion solution (DuPont). To produce the anode, catalyst ink consisting of aqueous dispersion of Pt_{50}–Ru_{50} black (Alfa Aesar), 5% Nafion solution and isopropanol was screen-printed on GDL and Nafion membrane surface. The cathode was formed by using catalyst ink that comprises aqueous dispersion of 40%Pt/C (BASF Fuel Cell), 5% Nafion solution and isopropanol. The resulted loadings for anode and cathode were 3.00 mg cm^{-2} and 3.50 mg cm^{-2}, respectively.

2.3. Characterization of PAH/PSS self-assembly layer containing Pt_{35}–Ru_{65}

PAH/PSS self-assembled on Nafion membrane was determined using the UV–visible spectroscopy (Jasco, V570) with scanning rate of 400 nm min^{-1} from 200 nm to 500 nm. The un-treated Nafion membrane was used as the reference. The surface morphology, composition of deposited Pt–Ru layer and thickness of PAH/PSS bi-layers were characterized by a field emission scanning electron microscope, FESEM (JEOLJSM-6700F), with an energy-dispersive spectrometer, EDS (OXFORD INSTRUMENTS, INCAx-sight 7557). Electron probe micro-analysis, EPMA (JEOL, JXA-8500F) was adopted to further confirm the compositions of deposited Pt–Ru layers. The PANalytical X-ray diffractometer X'Pert Pro using CuKα radiation source operating at 40 kV and 30 mA was used to investigate the X-ray diffraction (XRD) patterns of the PAH/PSS–Pt–Ru samples and the alloy phase of the deposited layer. Proton conductivities of PAH/PSS–Pt–Ru samples were determined through two probes AC method [28] using an impedance analyzer (EG&G model 5210 lock in amplifier). The membrane was cut in 3.50 cm × 3.50 cm dimensions and impedance measurements were performed in 97% RH at 55 °C. In-plane (lateral) proton conductivities (σ) were calculated by using the equation shown below.

$$\sigma = l/R_b A$$

Where $\boldsymbol{\sigma}$, proton conductivity of membrane (S cm^{-1}), l, thickness of membrane or distance between the two electrodes (cm), A, electrode area (cm^2), R_b, resistance of membrane.

The R_b values of Nafion-117 and PAH/PSS–Pt–Ru samples were 0.2697 Ω and 0.5803 Ω, respectively. These values were obtained through fitting of the curves shown in Fig. 9 using appropriate simulated circuit. The l in this study was 183 × 10^{-4} cm, which was the thickness of Nafion-117, and electrode area (A) was 5.309 cm^2.

2.4. Preparation and evaluation of MEA

The anode, PAH/PSS–Pt–Ru sample and cathode were placed at the position as shown in Fig. 1. Hot-pressing the sandwich structure with a pressure of 4 MPa at 139 °C for 90 s formed the MEAs, which was denoted as MEA–PAH/PSS–Pt–Ru. In order to compare the mitigation of methanol crossover and performance, we prepare a new MEA, denoted as normal-MEA, which comprises the Nafion membrane without any coating and having identical anode and cathode as that of MEA–PAH/PSS–Pt–Ru.

The MEAs were tested in a single cell test fixture (5 cm^2), supplied by Electrochem Inc., USA, with serpentine flow pattern on graphite plates. 2 M of methanol as anode fuel and dry oxygen gas as cathode fuel were fed into the anode and cathode with a flow rate of 1 ml min^{-1} and 400 sccm, respectively.

According to the results of H. T. Liu [34], the CO_2 concentration detected at the cathode exhaust were directly related to the amount of methanol crossover. This was because most crossed-over methanol reaching the cathode reacted with oxygen and turned into CO_2, and only a very small portion became the intermediate product CH_xO_y and CO [9,35]. The reaction equation at the cathode [9] is as below,

$$2CH_3OH + 3O_2 \rightarrow 2CO_2 + 4H_2O$$

The cathode exhaust may include liquid water ($H_2O(l)$), water vapor ($H_2O(v)$), methanol vapor ($CH_3OH(v)$), liquid methanol ($CH_3OH(l)$), oxygen (O_2), carbon dioxide (CO_2), carbon monoxide (CO), and CH_xO_y. An ice-trap was placed before the CO_2 sensor to trap water and methanol vapor for each experiment. The amount of collected methanol in an ice-trap and the amount of crossed-over methanol reacted to form CH_xO_y and CO is negligible in our experiment, verified by the gas chromatography method. Therefore, the rate of methanol crossover can be accurately determined through measuring CO_2 concentration at cathode exhaust via CO_2 sensor. All CO_2 concentration remained steady after 20 min into the test. The output current, voltage and the CO_2 concentrations were measured when the CO_2 concentration remained steady after 40 min.

3. Results and discussions

3.1. Characterization of PAH/PSS bi-layers containing Pt–Ru

Fig. 2 shows the UV–visible spectra of PAH/PSS–Pt^{+}–Ru^{+} sample. The diamond and square symbols represent the self-assembly of 5 and 10 bi-layers of PAH/PSS on the Nafion membrane surface, respectively. According to S.P. Jiang and coworkers [31], the sodium salt of polystyrene sulfonic acid in PSS was found at the characterized wavelength of 228 nm. In Fig. 2, we

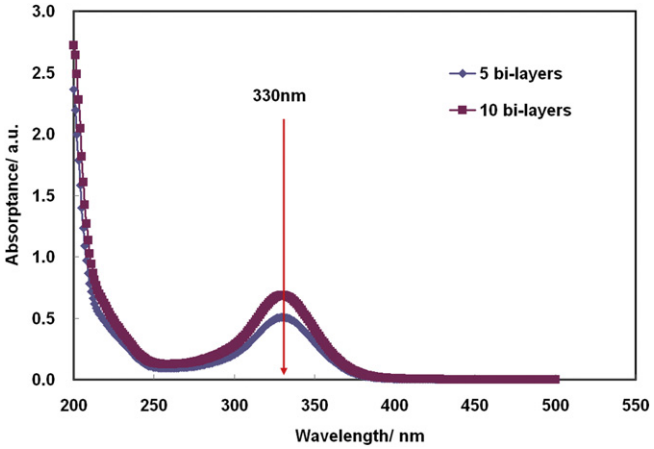

Fig. 2. UV–visible profiles for PAH/PSS–Pt^{+}–Ru^{+} samples.

observe strong absorbance at 330 nm and a very weak absorbance at 228 nm. The absorbance at 330 nm is most likely related to the characterized wavelength of Ru ions [36]. However, the characterized wavelength of Pt ions at 202 nm or 214 nm [37] was not found. Rather, the existence of Pt was confirmed by the XRD patterns of this sample in the reduction form (as shown below). Consequently, the sodium salt in the polystyrene sulfonic acid is almost completely replaced by Ru and Pt ions. Since the PAH is transparent in the UV–visible spectral range, the increase in the absorbance is ascribed to the deposition of PSS on the deposited layer. Therefore, the 10 PAH/PSS bi-layers show a higher absorbance at 330 nm than the 5 PAH/PSS bi-layers. The linear increase of absorbance at 330 nm indicates a regular growth of the deposited layer. After reduced with $NaBH_4$, the UV–visible profile of this sample is shown in Fig. 3. The absorbance at 330 nm disappeared and the sample showed a brown color, indicating that Ru and Pt ions were being reduced to produce the Ru and Pt metal.

XRD patterns of the PAH/PSS–Pt–Ru samples and Nafion-117 measured at X-ray incident angle of 1° are shown in Fig. 4. Comparing with the XRD patterns of Nafion-117 (as shown in Fig. 4(a)), there are no significant differences between the PAH/PSS–Pt–Ru sample with 5 bi-layers and Nafion membrane except the peak shows a 0.35° shift toward higher value. However, the XRD patterns of PAH/PSS–Pt–Ru samples with 10 and 15 bi-layers of PAH/PSS show sharp peaks at 40.35°, 46.85°, 68.25° and 82.05°. In order to verify the existence of Pt element and alloy phase, we prepare a PAH/PSS–Pt sample (10 bi-layers) that fabricated by the same conditions with PAH/PSS–Pt–Ru sample except the Pt ion is only exchanged in the PSS. Fig. 4(e) shows the XRD pattern of PAH/PSS–Pt sample. The peaks located at 39.80°, 46.34°, 67.69° and 81.55° correspond to Pt(111), Pt(200), Pt (220), Pt(311) faces, indicating the existence phase is a Pt element. Since only Pt and Ru ions present in the PAH/PSS bi-layers, one should only perform the XRD patterns of this two elements after the reduction reaction. Consequently, PAH/PSS–Pt–Ru samples have peak positions similar to that of the PAH/PSS–Pt, i.e. 40.35°, 46.85°, 68.25° and 82.05°, suggesting the existence of Pt element in these samples. The result of EDS further confirms the existence of Pt element in the PAH/PSS–Pt–Ru samples. Due to the absence of the characterized peak for Ru element at the peak position of Pt(111) face, the Pt(111) face peak at 39.80° is chosen as the reference peak to confirm the existence of alloy phase by comparing the lattice constants between the pure Pt and the obtained Pt–Ru sample. Bragg's equation yields a lattice constant of 3.920 Å for pure Pt and 3.855 Å for the obtained Pt–Ru sample. The lattice constant of the PAH/PSS–Pt–Ru sample is clearly smaller than that of the PAH/PSS–Pt

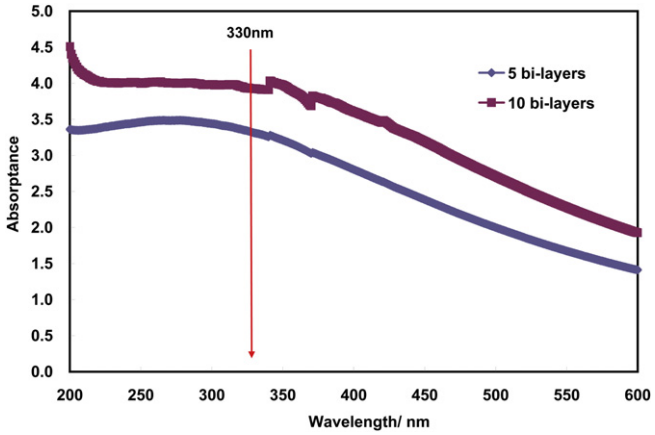

Fig. 3. UV–visible profiles for PAH/PSS–Pt–Ru samples.

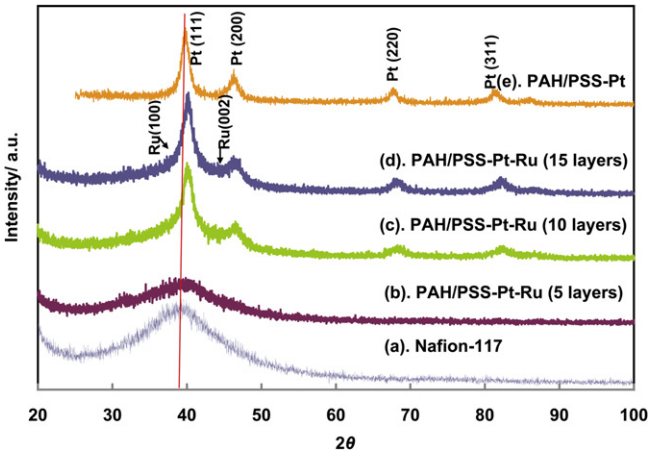

Fig. 4. XRD patterns of PAH/PSS–Pt–Ru, PAH/PSS–Pt and Nafion-117 membrane.

sample, suggesting that the deposited layer in the PAH/PSS self-assembly membrane is a Pt–Ru alloy. The substrate effect of the GID method prevents the determination of the composition of the thin film from the lattice parameters derived from the XRD. On the other hand, EPMA provides accurate measurement of the atomic ratio of thin film, and is applied to determine the composition of the thin film. The EPMA result (an average over 25 sampling points) demonstrates that the atomic ratio of Pt to Ru is 35:65. The EDS results (an average over 5 sampling surfaces) further confirm this atomic ratio. Therefore, the PAH/PSS–Pt–Ru sample with 5 bi-layers presents the Pt_{35}–Ru_{65} alloy phase. The grain size of this sample, calculated using Debye–Scherrer equation with the XRD data in Fig. 4, is nearly 12 nm – indicating the Pt_{35}–Ru_{65} catalyst is in nanometer-sized scale.

Fig. 5 shows the cross-sectional view of PAH/PSS–Pt–Ru sample with 30 bi-layers. Two different morphologies are observed and the upper layer measures a thickness of 525 nm. The result of EDS line scanning indicates the upper layer contains nitrogen, carbon, hydrogen, Pt and Ru elements but not the fluoride element. Obviously, upper layer is the PAH/PSS bi-layer which owns the thickness of 525 nm. Therefore, the average thickness of a PAH/PSS bi-layer is 17.5 nm and the thickness for 5 PAH/PSS bi-layers is 87.5 nm. It means that the 5 bi-layers of PAH/PSS–Pt–Ru sample have the self-

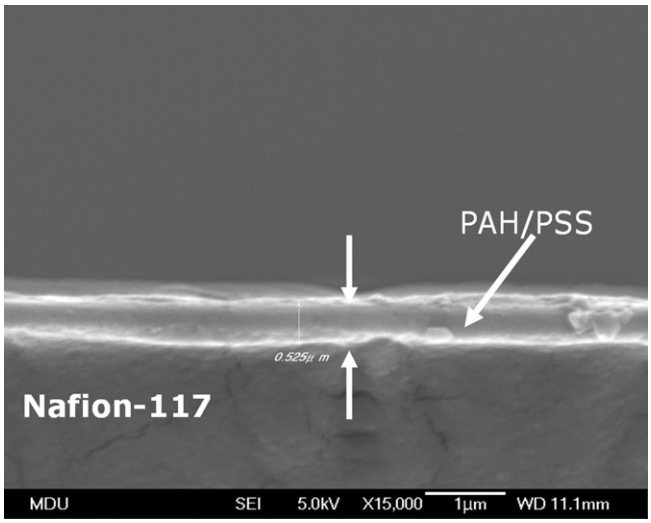

Fig. 5. Cross-sectional SEM view of PAH/PSS–Pt–Ru sample with 30 bi-layers.

assembled PAH/PSS layer with a thickness of 87.5 nm, consisting of Pt_{35}–Ru_{65} catalyst on both sides of Nafion membrane surface. The loading of Pt_{35}–Ru_{65} alloy in 5 PAH/PSS bi-layers is 0.46 μg cm^{-2}, determined using the TGA method [6].

Fig. 6 presents the cyclic voltammograms (CV) profile for 5 bi-layers of PAH/PSS–Pt–Ru sample measured in a solution of 0.50 M methanol and 0.50 M H_2SO_4 at a scanning rate of 50 mV s^{-1}. A small peak of methanol oxidation was found at the potential range of 0.38–0.84 V when carefully examined. The peak current density at 0.65 V is 2.5 × 10^{-3} mA cm^{-2} (5.43 A g^{-1}). This result indicates that the Pt_{35}–Ru_{65} deposited in the PAH/PSS bi-layers can oxidizes methanol and functions like a catalyst and an electrode with even a small amount of 0.46 μg cm^{-2}.

3.2. Methanol crossover and performance

Fig. 7 shows the CO_2 concentration measured at the cathode exhaust varies with according to the current density of MEA–PAH/PSS–Pt–Ru (5 bilayer) and normal-MEA at 80 °C, respectively. The diamond and square symbols represent the normal-MEA and MEA–PAH/PSS–Pt–Ru, respectively. The CO_2 concentrations of both MEAs decrease with increasing current density. This is because the methanol crossover is a combination of diffusion part ($-D^{\Delta}c/t$) and proton drag part ($(\lambda_m/nF)I$) [34] (the permeation caused by the pressure difference is negligible since the operating pressure on both sides are equal). At 80 °C, the diffusion part decreases with increasing current density because the methanol concentration in the anode catalyst layer decreases with increasing current density. Furthermore, the proton drag part decreases with increasing current density because λ_m is proportional to the methanol concentration at the interface between the electrolyte membrane and anode catalyst layer, which decreases with increasing current density. Therefore, the methanol crossover rate of MEA–PAH/PSS–Pt–Ru decreases with increasing current density, which has similar trends as normal-MEA, despite having additional 5 PAH/PSS bi-layers with Pt_{35}–Ru_{65} catalyst on Nafion surface.

In Fig. 7, the CO_2 concentrations of MEA–PAH/PSS–Pt–Ru are lower than that of the normal-MEA by 22% (on average). Fig. 8 presents the polarization curves of both MEAs operated at 80 °C. The open circuit voltage (OCV) of normal-MEA is 0.64 V, while the OCV of MEA–PAH/PSS–Pt–Ru is 0.68 V. It is known that the OCV of DMFC increases with the occurrence of mitigation of methanol crossover [6,38]. Therefore, the increment of OCV of 0.04 V for

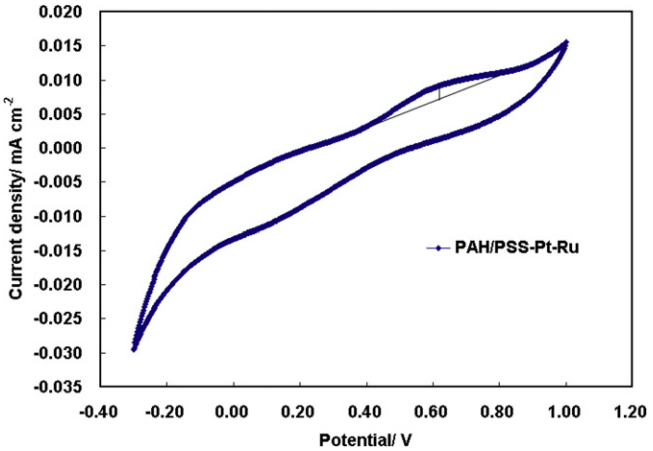

Fig. 6. CV profile for PAH/PSS–Pt–Ru sample with 5 bi-layers. (Testing in 0.50 M CH_3OH and 0.50 M H_2SO_4 solution at 25 °C).

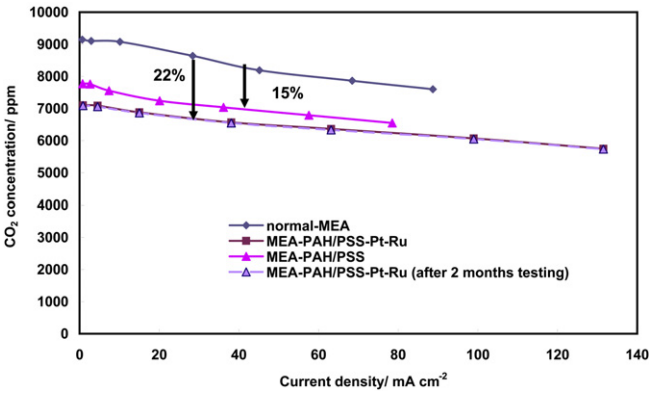

Fig. 7. CO_2 concentrations measured at cathode exhaust vs. current density for MEA–PAH/PSS–Pt–Ru, MEA–PAH/PSS and normal-MEA at 80 °C. (Anode fuel: 2 M methanol (1 ml min^{-1}); cathode fuel: O_2 (400 sccm); membrane: Nafion-117).

MEA–PAH/PSS–Pt–Ru is attributed to the mitigation of methanol crossover caused by the self-assembled PAH/PSS layer with Pt_{35}–Ru_{65} catalyst on Nafion membrane surface, which is consistent with the result in Fig. 7.

Fig. 8 demonstrates that the cell performance of MEA–PAH/PSS–Pt–Ru is better than that of normal-MEA. Comparing the power density (@0.30 V) and potential (@62.5 mA cm^{-2}) between the MEA–PAH/PSS–Pt–Ru and normal-MEA, the power density and potential gains are up to 48% and 22% for MEA–PAH/PSS–Pt–Ru, respectively. It suggests that the existence of PAH/PSS bi-layers with Pt_{35}–Ru_{65} catalyst on Nafion surface does suppress the methanol crossover and improve the cell performance significantly.

In order to clarify the effect of Pt_{35}–Ru_{65} catalyst in PAH/PSS self-assembly layer, we prepare a new MEA, denoted as MEA–PAH/PSS, consisting of only self-assembly PAH/PSS bi-layers (5 bi-layers) on Nafion surface with identical anode and cathode as the MEA–PAH/PSS–Pt–Ru. Fig. 7 shows that the CO_2 concentration of MEA–PAH/PSS is about 15% lower than that of normal-MEA. In Fig. 8, the OCV of MEA–PAH/PSS is 0.66 V, which is higher than that of normal-MEA by 0.02 V. However, the output cell performance (based on the potential gain) of MEA–PAH/PSS is lower than that of normal MEA by about 6%. These results suggest that the presence of PAH/PSS self-assembly layer on Nafion surface does mitigate the methanol crossover and also decrease the cell performance due to the increase of proton transfer resistance. It is consistent with the result of Deligoz [28] as the existence of PAH/PSS self-assembly layer reduces the methanol permeability at the expense of the

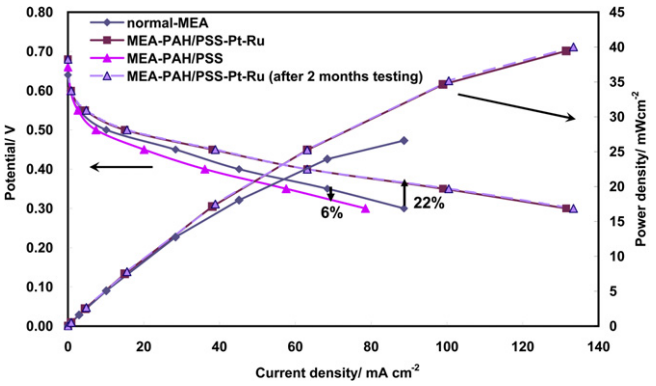

Fig. 8. Polarization curves and power density of MEA–PAH/PSS–Pt–Ru, MEA–PAH/PSS and normal-MEA at 80 °C. (Anode fuel: 2 M methanol (1 ml min^{-1}); cathode fuel: O_2 (400 sccm); membrane: Nafion-117).

proton conductivity of Nafion membrane. Comparing the CO_2 concentration and output cell performance between the MEA–PAH/PSS and MEA–PAH/PSS–Pt–Ru, the MEA–PAH/PSS–Pt–Ru shows 7% lower CO_2 concentration than the MEA–PAH/PSS and the output cell performance is better than that of normal MEA (power density improvement of 48% @0.30 V; potential gain of 22% @62.5 mA cm^{-2}) and MEA–PAH/PSS. Since the only difference between MEA–PAH/PSS and MEA–PAH/PSS–Pt–Ru is the Pt_{35}–Ru_{65} in PAH/PSS self-assembly layer, the improvement of cell performance and mitigation of methanol crossover are related to the existence and reaction of Pt_{35}–Ru_{65} catalyst in PAH/PSS.

The most probable mechanism through which can explain the above results is the deposited Pt_{35} Ru_{65} catalyst in the PAH/PSS bi-layers reacts with the crossed-over methanol and produces electrons, protons and CO_2, i.e. $CH_3OH + H_2O \rightarrow CO_2 + 6e^- + 6H^+$. This will reduce the amount of methanol crossover and mixed potential effect at the cathode. Furthermore, due to the nanometer-sized thickness of deposited Pt_{35}–Ru_{65} catalyst in PAH/PSS bi-layers, the anode Pt_{50}–Ru_{50} catalyst layer will be embedded into the PAH/PSS bi-layers through the formation of MEA by hot-pressing process. This provides the electrons a transfer media to the external circuit. It means that the electrons that produced by the reaction of crossed-over methanol over the deposited Pt_{35}–Ru_{65} in the PAH/PSS bi-layers can be transferred to the external circuit through the embedded anode catalyst layer, offering extra electrons to the external circuit. The protons that produced by the reaction of crossed-over methanol are conducted to the cathode via the PAH/PSS and Nafion membrane, and provide extra current. Moreover, the Nafion-117 consisting of 5 PAH/PSS bi-layers shows lower methanol permeability compared to that of the un-modified Nafion-117, i.e. 4.88×10^{-7} vs. 6.04×10^{-7} cm^2 s^{-1} at 30 °C [28]. The effect of pore plugging of the membrane [38] by the Pt_{35}–Ru_{65} deposition on the PAH/PSS bi-layers also contributed to the mitigation of methanol crossover. However, the deposition of 5 PAH/PSS bi-layers with Pt_{35}–Ru_{65} catalyst on the Nafion surface reduces the proton conductivity of Nafion-117 from 12.78 to 5.94 mS cm^{-1} at 55 °C (as shown in Fig. 9). This indicates that the presence of PAH/PSS bi-layers with Pt_{35}–Ru_{65} catalyst on Nafion membrane increases the resistance of membrane and reduces the cell performance. In fact, the output power density and potential have been improved at 80 °C by 48% (@0.30 V) and 22% (@62.5 mA cm^{-2}) (as shown in Fig. 8), respectively. The evidence supports the inference that the performance improvement caused by the reduction of mixed potential effect and the extra current produced by the deposited Pt_{35}–Ru_{65} in the PAH/PSS bi-layers are higher than the performance reduction resulted from the decrease of proton conductivity. Therefore, the 5 PAH/PSS bi-layers with Pt_{35}–Ru_{65} catalyst self-assembled on both sides of the Nafion surface function as a methanol filter and a barrier that reacts and blocks the crossed-over methanol. The proposed mechanism is shown in Fig. 10.

In order to verify the above inference, we compare the reduction of methanol crossover current and the actual output current increment between the MEA–PAH/PSS–Pt–Ru and normal-MEA. The methanol crossover current is defined as the equivalent current that produced by the crossed-over methanol, calculate using the below equation from the CO_2 data (based on the reaction equation: $2\,CH_3OH + 3O_2 \rightarrow 2CO_2 + 4H_2O$) in Fig. 7.

$$J(CH_3OH) = QX_{CO_2}\,P/5\left(1.036 \times 10^{-4}\right)RT$$

Where $J(CH_3OH)$, the methanol crossover current (mA cm^{-2}), Q, cathode flow rate $Q = Q_{CO_2} + Q_{O2} + Q_{H_2O}$ (sccm), X_{CO_2}, carbon dioxide concentration at cathode exit (ppm $\times$ 10^{-6}), Q_{O_2}, oxygen flow rate (sccm), Q_{CO_2}, carbon dioxide flow rate (sccm), Q_{H_2O}, water vapor flow rate (sccm), P, pressure at cathode exit (atm), R, gas constant, T, temperature in K at the CO_2 sensor position.

Calculation of methanol crossover current at the current density of 62.5 mA cm^{-2} yields a reduction of methanol crossover current of 40.6 mA cm^{-2} for MEA–PAH/PSS–Pt–Ru. In contrast, the output current density measured from polarization curves of MEA–PAH/PSS–Pt–Ru at 0.30 V is 92.6 mA cm^{-2}, which yields an increment of 30.1 mA cm^{-2} when compared to the normal-MEA (62.5 mA cm^{-2} @0.30 V). This indicates that the amount of reduction of methanol crossover current almost completely transferred to the output current density (30.1 mA cm^{-2}), and only a small amount of crossover current (10.5 mA cm^{-2}) is consumed by the increased resistance. It means that the performance improvement is greater than the performance reduction caused by the reduced proton conductivity. This analysis supports the above inference.

To study the stability of MEA–PAH/PSS–Pt–Ru, continuous operation of this MEA under the conditions similar to that described in the experimental sections was performed and monitored for two months. As shown in Figs. 7 and 8, the suppression of methanol crossover and cell performance remains unchanged. The result indicates that the additional PAH/PSS self-assembly bi-layers containing Pt_{35}–Ru_{65} is stable after 2 months of continuous tests.

Note that there are significant differences between the structure of proton exchange membrane (PEM) in this study and the

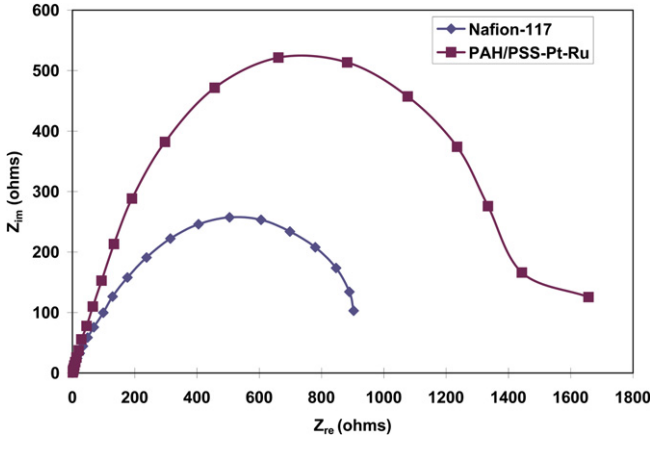

Fig. 9. Nyquist plots of PAH/PSS–Pt–Ru sample with 5 bi-layers and Nafion-117.

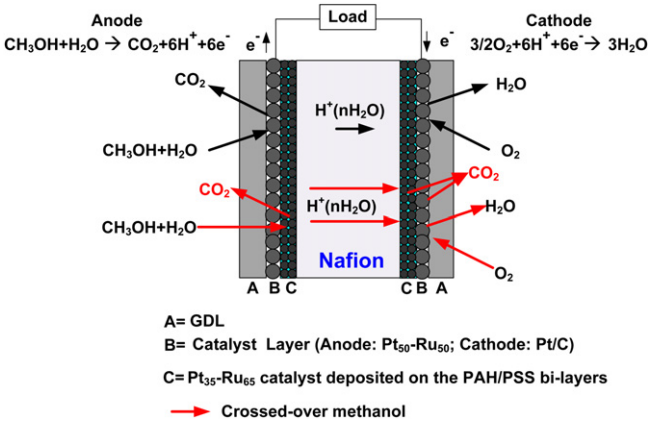

Fig. 10. Diagram of the proposed mechanism of mitigation of methanol crossover for Nafion surface self-assembled with 5 PAH/PSS bi-layers consisting of Pt_{35}–Ru_{65} catalyst.

structure of PEM in the previous study developed by our laboratory [6]. As mentioned above, the PEMs reported in this study have a layer of nanometer-sized Pt_{35}–Ru_{65} catalyst deposited in the PAH/PSS bi-layers on both sides of Nafion-117. In contrast, the PEMs in previous study have a layer of nanometer-sized Pt_{37}–Ru_{63}/Pt or Pt_{37}–Ru_{63}/Pt_{20}–Ru_{80} particles directly deposited on the surface of PEM anode. Furthermore, the loading and thickness of the deposited Pt_{35}–Ru_{65} catalyst in this study is smaller and thinner than that of the previous study, i.e. 0.46 μg cm^{-2} vs. 0.52 mg cm^{-2} and 87.5 nm vs. 3.0 μm. Finally, the nanometer-sized catalyst in this study is Pt_{35}–Ru_{65} catalyst as opposed to a highly concentrated double Pt_{37}–Ru_{63}/Pt_{20}–Ru_{80} or Pt_{37}–Ru_{63}/Pt particles catalyst layers in the previous' PEM. There is a significant performance improvement of 22% in this study as opposed to the 18% in the previous study although only 0.46 μg cm^{-2} of Pt_{35}–Ru_{65} catalyst is used. The performance improvement is mainly due to the lesser and thinner deposited Pt–Ru, and the deposition of Pt–Ru catalyst in the additional PAH/PSS layer without sacrificing the proton conductivity of Nafion. These effects reduce the resistance caused by the deposition of Pt–Ru catalyst onto the Nafion membrane compared to the Pt–Ru directly deposited on the surface of PEM anode in the previous study.

4. Conclusions

Nanometer-sized Pt_{35}–Ru_{65} catalyst with layer thickness of 87.5 nm have been successfully self-assembled through 5 PAH/PSS bi-layers onto both side of Nafion surface using the LbL technique under the designed experimental conditions. The layer thickness of Pt_{35}–Ru_{65} catalyst is determined by the number of deposited PAH/PSS layers and the concentrations of Pt and Ru ions in PSS solution. This composite Nafion membrane with Pt_{35}–Ru_{65} loading of 0.46 μg cm^{-2} could suppress methanol crossover by 22% (on average) and improve power density as well as the potential by 48% (@0.30 V) and 22% (@62.5 mA cm^{-2}) at 80 °C, respectively. This is because the Pt_{35}–Ru_{65} catalyst in PAH/PSS has the capability to oxidize the crossed-over methanol and functions like an electrode and methanol filter. It is believed that the crossed-over methanol flows through the Pt_{35}–Ru_{65} catalyst in PAH/PSS to produce electrons, protons and CO_2. The produced electrons are conducted to the external circuit through the embedded anode Pt_{50}–Ru_{50} catalyst layer, while the protons are transferred to the cathode via the PAH/PSS and Nafion membrane. These provide extra current to the external circuit. Furthermore, both the reaction of crossed-over methanol over Pt_{35}–Ru_{65} catalyst and the introducing of low methanol permeability of PAH/PSS layer reduce the amount of crossed-over methanol and mixed potential effect at the cathode. As a result, it mitigates the methanol crossover and improves the performance although the deposition of Pt_{35}–Ru_{65} and PAH/PSS bi-layers on Nafion decreases the proton conductivity. Due to the lesser and thinner deposited Pt_{35}–Ru_{65} and the Pt_{35}–Ru_{65} layer deposited in the additional PAH/PSS layer without sacrificing the proton conductivity of Nafion membrane, the performance improvement obtained is 22% in this study as opposed to the 18% in the previous study although only 0.46 μg cm^{-2} of Pt_{35}–Ru_{65} catalyst with layer thickness of 87.5 nm is used.

Acknowledgment

The authors wish to acknowledge the National Science Council of Taiwan (R.O.C) for the financial support under the grant number of NSC 99-2221-E-451 -014 -MY2.

References

[1] F. Barbir, PEM Fuel Cells: Theory and Practice, Elsevies Inc., USA, 2005, ISBN 012-078142-5.
[2] L.C. Cogo, M.V. Batisti, M.A. Pereira-da-Silva, O.N. Oliveira Jr., F.C. Nart, F. Huguenin, J. Power Sources 158 (2006) 160–163.
[3] J.Y. Park, J.H. Lee, S.K. Kang, J.H. Sauk, I. Song, J. Power Sources 178 (2008) 181–187.
[4] A. Heinzel, V.M. Barragan, J. Power Sources 84 (1999) 70–74.
[5] G.T. Burstein, C.J. Barnett, A.R. Kucernak, K.R. Williams, Catal. Today 38 (1997) 425–437.
[6] C.H. Wan, C.H. Lin, J. Power Sources 186 (2009) 229–237.
[7] J.S. Wainright, D. Wang, R.F. Weng, M. Savinell, J. Electrochem. Soc. 142 (1995) L121–L123.
[8] M. Weng, J.S. Wainright, U. Landau, R.F. Savinell, J. Electrochem. Soc. 143 (1996) 1260–1263.
[9] J.T. Wang, S. Wasmus, R.F. Savinell, J. Electrochem. Soc. 143 (1996) 1233–1239.
[10] S. Wasmus, J.T. Wang, R.F. Savinell, J. Electrochem. Soc. 142 (1995) 3825–3833.
[11] P. Xing, G.P. Robertson, M.D. Guiver, S.D. Mikhailenko, S. Kaliaguine, Polymer 46 (2005) 3257–3263.
[12] F. Wang, M. Hickner, Y.S. Kim, T.A. Zawodzinski, J. McGrath, J. Membr. Sci. 197 (2002) 231–242.
[13] H. Bai, W.S. Winston Ho, J. Membr. Sci. 313 (2008) 75–85.
[14] M.A. Hickner, H. Ghassemi, Y.S. Kim, B.R. Einsla, J.E. McGrath, Chem. Rev. 104 (2004) 4587–4612.
[15] C. Yang, S. Srinivasan, A.S. Arico`, P. Creti, V. Baglio, V. Antonucci, Electrochem. Solid-State Lett. 4 (2001) A31–A34.
[16] N. Miyake, J.S. Wainright, R.F. Savinell, J. Electrochem. Soc. 148 (2001) A905–A909.
[17] P. Staiti, A.S. Aricò, V. Baglio, F. Lufrano, E. Passalacqua, V. Antonucci, Solid State Ionics 145 (2001) 101–107.
[18] V. Tricoly, J. Electrochem. Soc. 145 (1998) 3798–3801.
[19] J. Liu, H. Wang, S. Cheng, K.Y. Chan, J. Membr. Sci. 246 (2005) 95–101.
[20] C. Pu, W. Huang, K.L. Ley, E.S. Smoktin, J. Electrochem. Soc. 142 (1995) L119–L120.
[21] Z.Q. Ma, P. Cheng, T.S. Zhao, J. Membr. Sci. 215 (2003) 327–336.
[22] Z.X. Liang, T.S. Zhao, J. Phys. Chem. C 111 (2007) 8128–8134.
[23] C.H. Wan, C.L. Chen, Int. J. Hydrogen Energy 34 (2009) 9515–9522.
[24] C.H. Wan, J.M. Wei, M.T. Lin, C.H. Lin, Int. J. Electrochem. Sci. 6 (2011) 889–900.
[25] H. Uchida, Y. Mizuno, M. Watanabe, J. Electrochem. Soc. 149 (2002) A682–A687.
[26] A.A. Argun, J.N. Ashcraft, P.T. Hammond, Adv. Mater. 20 (2008) 1539–1543.
[27] S. Yılmaztürk, H. Deligöz, M. Yılmazoğlu, H. Damyan, F. Öksüzömer, Karaca, S. Naci Koc, A. Durmus, M. Ali Gürkaynak, J. Power Sources 195 (2010) 703–709.
[28] H. Deligöz, S. Yılmaztürk, T. Karaca, H. Özdemir, S. Naci Koc, F. Öksüzömer, A. Durmus, M. Ali Gürkaynak, J. Membr. Sci. 326 (2009) 643–649.
[29] H. Lin, C. Zhao, W. Ma, H. Li, H. Na, Int. J. Hydrogen Energy 34 (2009) 9795–9801.
[30] S. Mu, H. Tang, Z. Wan, M. Pan, R. Yuan, Electrochem. Commun. 7 (2005) 1143–1147.
[31] S.P. Jiang, Z. Liu, Z.Q. Tian, Adv. Mater. 18 (2006) 1068–1072.
[32] T.R. Farhat, P.T. Hammond, Adv. Funct. Mater. 16 (2006) 433–444.
[33] H. Deligöz, S. Yılmaztürk, M. Yılmazoğlu, H. Damyan, J. Membr. Sci. 351 (2010) 131–140.
[34] J.H. Han, H.T. Liu, J. Power Sources 164 (2007) 166–173.
[35] A.S. Aricò, P. Cretì, P.L. Antonucci, V. Antonucci, Electrochem. Solid-State Lett. 1 (1998) 66–68.
[36] P. Castillo-Villalón, J. Ramırez, M.J. Peltre, C. Louis, P. Massiani, Phys. Chem. Chem. Phys. 6 (2004) 3739–3746.
[37] T. Lopez, M. Villa, R. Comez, J. Phys. Chem. 95 (1991) 1690–1693.
[38] X. Li, E.P.L. Roberts, S.M. Holmes, J. Power Sources 154 (2006) 115–123.